



The following Communications have been judged by at least two referees to be “very important papers” and will be published online at www.angewandte.org soon:

X. Lang, H. Ji, C. Chen, W. Ma,* J. Zhao*

Selective Formation of Imines by Aerobic Photocatalytic Oxidation of Amines on TiO₂

R. P. Sonawane, V. Jheengut, C. Rabalakos, R. Larouche-Gauthier, H. K. Scott, V. K. Aggarwal*

Enantioselective Construction of Quaternary Stereogenic Centers from Tertiary Boronic Esters: Methodology and Applications

K. Press, A. Cohen, I. Goldberg, V. Venditto, M. Mazzeo, M. Kol*

Salalen–Titanium Complexes for the Highly Isospecific Polymerization of 1-Hexene and Propylene

K. Nakano, S. Hashimoto, M. Nakamura, T. Kamada, K. Nozaki*
Synthesis of Stereogradient Poly(propylene carbonate) by Stereo- and Enantioselective Copolymerization of Propylene Oxide with Carbon Dioxide

K. Ohmori, T. Shono, Y. Hatakoshi, T. Yano, K. Suzuki*

An Integrated Synthetic Strategy for Higher Catechin Oligomers

L. Aboshyan-Sorgho, C. Besnard, P. Pattison, K. R. Kittilstved, A. Aebischer, J.-C. Bünzli, A. Hauser,* C. Piguet*

Molecular Near-Infrared to Visible Light Upconversion in a Trinuclear d–f–d Complex

A. Donazzi, D. Livio, M. Maestri, E. Tronconi, A. Beretta,* G. Groppi, P. Forzatti

Synergy of Homogeneous and Heterogeneous Processes Probed by In Situ Spatially Resolved Measurements of Temperature and Composition

C. A. Naini, S. Franzka, S. Frost, M. Ulbricht, N. Hartmann*

Probing the Intrinsic Switching Kinetics of Ultrathin Thermoresponsive Polymer Brushes



“The three things I would take to a desert island would be a bed, a hunter, and a chef.

My favorite author (fiction) is Penelope Fitzgerald, who is a superb wordsmith ...”

This and more about Mike Hannon can be found on page 3114.

Author Profile

Mike Hannon _____ 3114



L. Bogani



G. Fernández



S. Inoue



E. N. Jacobsen

News

Sofja Kovalevskaja Award:

L. Bogani, S. Inoue, and G. Fernández _____ 3115

Ryoji Noyori Prize:

E. N. Jacobsen _____ 3115

John Bennett Fenn

Obituaries

M. N. Eberlin _____ 3116

Molecular Materials

Duncan W. Bruce, Dermot O'Hare, Richard I. Walton

Books

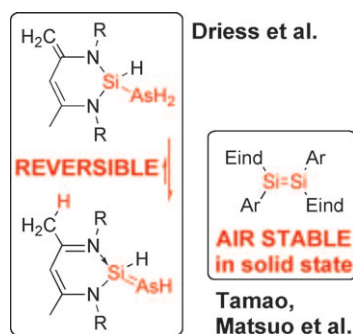
reviewed by D. Gatteschi _____ 3117

Highlights

Silicon Double Bonds

D. Scheschkewitz* — 3118–3119

Reversible Formation of a Blue Arsilene and Isolation of Air-Stable Emissive Disilenes



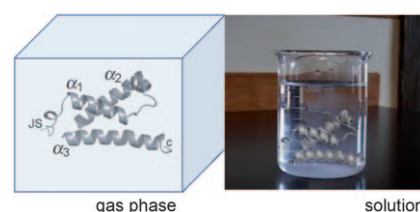
Two major breakthroughs in the chemistry of silicon compounds with double bonds have been reported recently: the reaction of a zwitterionic silylene with arsane yields the blue donor-stabilized arsilene with an As=Si bond (see left picture). Secondly, the extremely bulky and rigid hydrindacenyl substituent Eind allows for the preparation of emissive disilenes that are stable in the solid state towards air and moisture (right picture).

Protein-Structure Determination

P. E. Barran* — 3120–3122

(Re)Solution of a Protein Fold Without Solution

Who needs water? The gas phase may seem an esoteric place to examine the structures of proteins, but a new study reveals that the solution fold of the protein KIX can be retained for significant time periods in a mass spectrometer. Once in this ideal laboratory environment, details of the higher order fold can be elucidated at the single amino acid level.



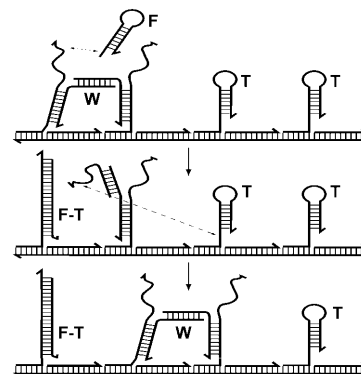
Reviews

Molecular Functional Units

Y. Krishnan, F. C. Simmel* — 3124–3156

Nucleic Acid Based Molecular Devices

Nucleic acid power: Molecular machines and devices made from DNA or RNA are becoming more complex and more versatile. Nucleic acids have been shown to be an exquisite material for the rational design of simple molecular switches, and researchers now envision the realization of molecular robots for nanotechnology, computers, as well as nanomachines that operate in vivo.



For the USA and Canada: ANGEWANDTE CHEMIE International Edition (ISSN 1433-7851) is published weekly by Wiley-VCH, PO Box 191161, 69451 Weinheim, Germany. Air freight and mailing in the USA by Publications Expediting Inc., 200 Meacham Ave., Elmont, NY 11003. Periodicals

postage paid at Jamaica, NY 11431. US POST-MASTER: send address changes to *Angewandte Chemie*, Journal Customer Services, John Wiley & Sons Inc., 350 Main St., Malden, MA 02148-5020. Annual subscription price for institutions: US\$ 9442/8583 (valid for print and electronic / print or electronic delivery); for

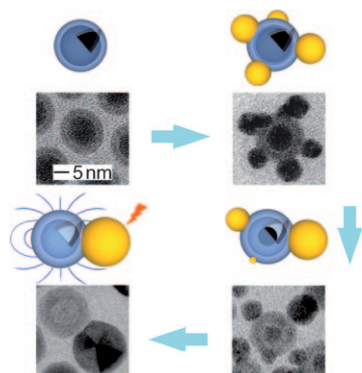
individuals who are personal members of a national chemical society prices are available on request. Postage and handling charges included. All prices are subject to local VAT/sales tax.

Communications

Hybrid Nanoparticles

S. Peng, C. Lei, Y. Ren, R. E. Cook,
 Y. Sun* 3158–3163

Plasmonic/Magnetic Bifunctional
 Nanoparticles

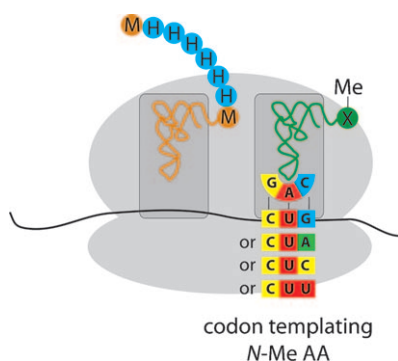


Superparafagilistic: An amorphous seed-mediated strategy has been developed for the synthesis of hybrid nanoparticles (see images) that are composed of silver (yellow) and iron oxide (blue) nanodomains and exhibit unique optical properties. These properties originate from both the strong surface plasmon resonance of the silver and the strong superparamagnetic responses of the iron oxide nanodomains.

N-Methyl Amino Acids

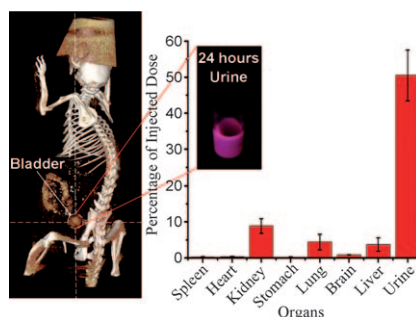
A. O. Subtelny, M. C. T. Hartman,
 J. W. Szostak* 3164–3167

Optimal Codon Choice Can Improve the
 Efficiency and Fidelity of N-Methyl Amino
 Acid Incorporation into Peptides by
 In-Vitro Translation



May the best codon win: N-methyl amino acids (N-Me AAs) are important modifications found in several nonribosomal peptide therapeutics. Previously, it was shown that three N-Me AAs are efficiently incorporated into peptides using a cell-free in-vitro translation system. Now, the incorporation of these N-Me AAs has been optimized by varying the template codon.

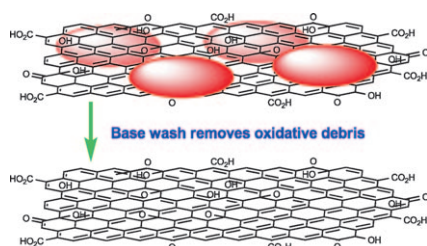
Going to waste: Renal clearance of 2 nm glutathione-coated luminescent gold nanoparticles (GS-AuNPs) was more than 10 to 100 times better than that of the similarly sized nonluminescent AuNPs coated by bis(*p*-sulfonatophenyl)phenylphosphine and cysteine. Urinary excretion of the particles was imaged with X-ray computed tomography (see picture of a mouse after injection of GS-AuNPs) and luminescence techniques in real time.



Nanoparticles

C. Zhou, M. Long, Y. Qin, X. Sun,*
 J. Zheng* 3168–3172

Luminescent Gold Nanoparticles with
 Efficient Renal Clearance



It'll come out in the wash! Graphene oxide has been shown to be a stable complex of oxidative debris (red ellipses in the picture) strongly adhered to functionalized graphene-like sheets. Under basic conditions the oxidative debris is stripped from the graphene-like sheets, and the resulting graphene oxide is conducting and cannot easily be resuspended in water.

Graphene Oxide

J. P. Rourke,* P. A. Pandey, J. J. Moore,
 M. Bates, I. A. Kinloch, R. J. Young,
 N. R. Wilson* 3173–3177

The Real Graphene Oxide Revealed:
 Stripping the Oxidative Debris from the
 Graphene-like Sheets



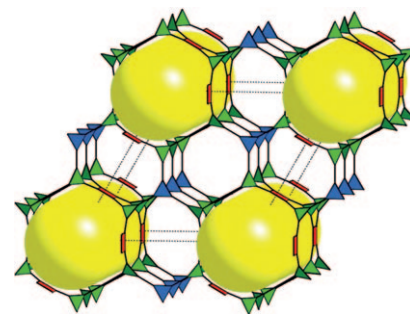
Metal–Organic Frameworks

Z. Guo, H. Wu, G. Srinivas, Y. Zhou,
S. Xiang, Z. Chen, Y. Yang, W. Zhou,*
M. O’Keeffe, B. Chen* — 3178–3181



A Metal–Organic Framework with
Optimized Open Metal Sites and Pore
Spaces for High Methane Storage at
Room Temperature

Holey MOF! Open copper sites and optimal pore spaces in UTSA-20 (see picture), a MOF based on the novel trinodal (3,3,4) net, has made UTSA-20 into the material with the highest methane storage density (0.22 g cm^{-3}) in micropores, and one of the few porous MOFs with storage volume capacity ($195 \text{ cm}^3 \text{ cm}^{-3}$) surpassing the DOE methane target of $180 \text{ cm}^3 \text{ cm}^{-3}$ at room temperature and 35 bar.



Luminescence

C.-H. Lin, Y.-Y. Chang, J.-Y. Hung, C.-Y. Lin,
Y. Chi,* M.-W. Chung, C.-L. Lin,
P.-T. Chou,* G.-H. Lee, C.-H. Chang,*
W.-C. Lin — 3182–3186



Iridium(III) Complexes of a
Dicyclopentylated Phosphite Tripod
Ligand: Strategy to Achieve Blue
Phosphorescence Without Fluorine
Substituents and Fabrication of OLEDs



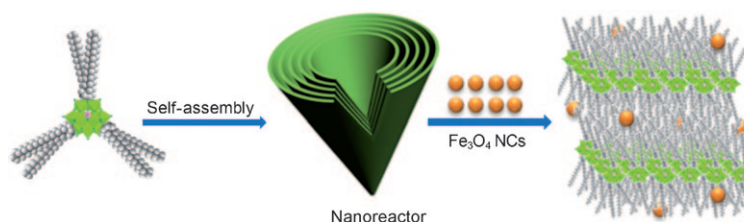
Toss the F: A new series of Ir^{III} complexes functionalized with pyridyltriazolate chromophores and a tripodal dicyclopentylated phosphite achieved highly efficient blue phosphorescence without employing any fluorine substituents. OLEDs with dopant [Ir(P^{^C}₂)(bptz)(PMe₂Ph)] (see structure; bptz = 3-*tert*-butyl-5-(2-pyridyl)-1,2,4-triazolate; P^{^C}₂ = dicyclopentylated phosphite tripod) show outstanding performance.

Heterogeneous Catalysis

A. Nisar, Y. Lu, J. Zhuang,
X. Wang* — 3187–3192



Polyoxometalate Nanocone
Nanoreactors: Magnetic Manipulation
and Enhanced Catalytic Performance



Magnetic personality: Nanocone nanoreactors consisting of polyoxometalates functionalized with surfactant alkyl chains and magnetite nanocrystals (NCs) provide enhanced catalytic performance for

the oxidation of sulfides to sulfones by a trap–release mechanism and advanced catalyst recovery under an external magnetic field.



A robust, inexpensive, and efficient photocatalytic system consisting of an artificial water-soluble [FeFe]-H₂ase mimic **1**, CdTe quantum dots, and ascorbic acid (H₂A), for H₂ production in pure water at room temperature has been developed. With this system, 786 μmol (17.6 mL) H₂ were obtained after 10 h irradiation ($\lambda > 400 \text{ nm}$) with TON up to 505 and TOF up to 50 h^{-1} under optimized conditions.

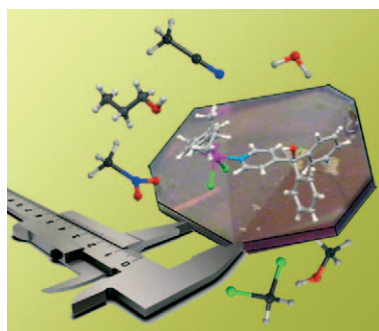
Hydrogenases

F. Wang, W.-G. Wang, X.-J. Wang,
H.-Y. Wang, C.-H. Tung,
L.-Z. Wu* ————— **3193–3197**

A Highly Efficient Photocatalytic System for Hydrogen Production by a Robust Hydrogenase Mimic in an Aqueous Solution



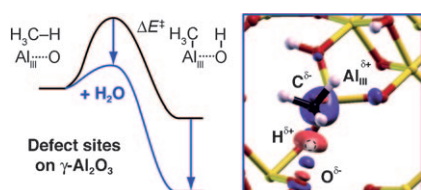
Backtracking the effect to the cause: The direct measure of the morphology of an organometallic molecular crystal can be used to rank experimentally the supramolecular synthons active in the packing and to estimate the solvation energies of the single crystallographic faces.



Crystallography

A. Bacchi,* G. Cantoni, D. Cremona,
P. Pelagatti, F. Uguzzoli — **3198–3201**

Exploration of Supramolecular Synthons and Molecular Recognition Starting from Macroscopic Measurements of Crystal Dimensions

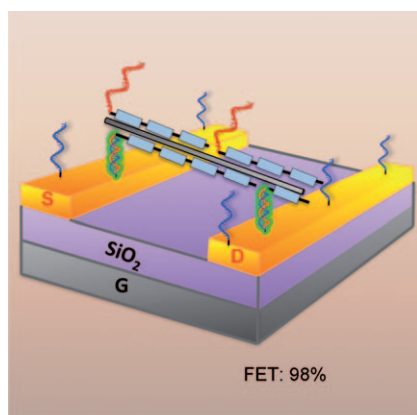


A low OH coverage, resulting from pre-treatment at 700°C , generates metastable three-coordinate Al_{III} sites and reactive (Al_{III},O) Lewis acid–base pairs on γ -alumina. Water plays a dual role by increasing the basicity of oxygen atoms without affecting the Lewis acidity of the Al_{III} sites and by stabilizing the metastable (110) termination, where these sites exist.

Methane Activation

R. Wischert, C. Copéret,* F. Delbecq,
P. Sautet* ————— **3202–3205**

Optimal Water Coverage on Alumina: A Key to Generate Lewis Acid–Base Pairs that are Reactive Towards the C–H Bond Activation of Methane



DNA block copolymer doing it all: A potentially scalable self-assembly method for single-walled carbon nanotubes (SWNTs) involves the use of amphiphilic DNA block copolymers. One such hybrid is able to cover the entire area of solution-based SWNT technologies, from selective dispersion to nondestructive functionalization to high-yield device fabrication such as field-effect transistors (see picture; S: source, G: gate, D: drain electrode).

Self-Assembly

M. Kwak, J. Gao, D. K. Prusty, A. J. Musser,
V. A. Markov, N. Tombros, M. C. A. Stuart,
W. R. Browne, E. J. Boekema,
G. ten Brinke, H. T. Jonkman,
B. J. van Wees, M. A. Loi,*
A. Herrmann* ————— **3206–3210**

DNA Block Copolymer Doing It All: From Selection to Self-Assembly of Semiconducting Carbon Nanotubes

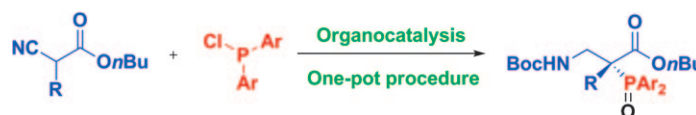


Asymmetric Synthesis

M. Nielsen, C. B. Jacobsen,
K. A. Jørgensen* — 3211–3214



Asymmetric Organocatalytic Electrophilic Phosphination



Meeting the challenge: The first asymmetric catalytic C*–P bond formation employing electrophilic phosphorus compounds has been developed using a catalytic amount of a dimeric cinchona alkaloid, and a subsequent one-pot process to deliver high stereoselectivities and

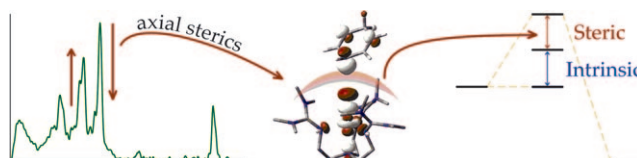
good yields of α -quaternary α -phosphino β -amino acids (see scheme). ^{31}P NMR experiments suggest a novel reaction mechanism wherein a cinchona alkaloid nucleophilically activates the phosphorus electrophile.

Reaction Barriers

S. D. Wong, C. B. Bell, III, L. V. Liu,
Y. Kwak, J. England, E. E. Alp, J. Zhao,
L. Que, Jr.,* E. I. Solomon* — 3215–3218



Nuclear Resonance Vibrational Spectroscopy on the $\text{Fe}^{\text{IV}}=\text{O}$ $S=2$ Non-Heme Site in TMG_3tren : Experimentally Calibrated Insights into Reactivity



Dissecting the barrier: The nuclear resonance vibrational spectrum of the $S=2$ $[(\text{TMG}_3\text{tren})\text{Fe}^{\text{IV}}=\text{O}]$ complex revealed features indicative of an axial “steric wall” that contributes to the overall reaction barrier. DFT calculations show that both

$S=2$ (axial attack) and $S=1$ (equatorial attack) surfaces possess steric contributions to their barriers, and estimates of these steric effects result in comparable intrinsic barriers for both spin surfaces (see picture).

Marine Natural Products

I. Paterson,* S. M. Dalby, J. C. Roberts,
G. J. Naylor, E. A. Guzmán, R. Isbrucker,
T. P. Pitts, P. Linley, D. Divlianska,
J. K. Reed, A. E. Wright* — 3219–3223



Leiodermatolide, a Potent Antimitotic Macrolide from the Marine Sponge *Leiodermatium* sp.

From the deep: Leiodermatolide is a structurally unique macrolide isolated from the deep-water marine sponge *Leiodermatium* sp. which exhibits potent antiproliferative activity against a range of human cancer cell lines and drastic effects on spindle formation in mitotic cells. Its unprecedented polyketide skeleton and stereochemistry were established using a combination of experimental and computational NMR methods.

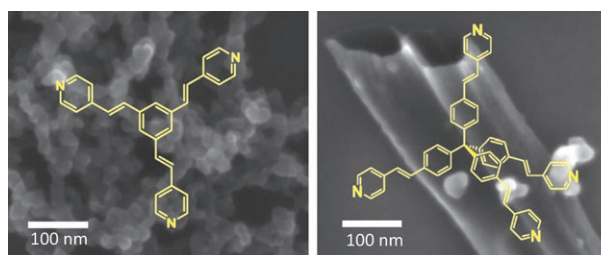


Nanotube Assembly

R. Kaminker, R. Popovitz-Biro,
M. E. van der Boom* — 3224–3226

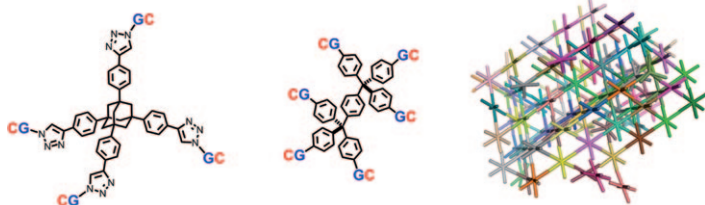


Coordination-Polymer Nanotubes and Spheres: A Ligand-Structure Effect



Ball or tube: Flexible and amorphous nanotubes were generated with a palladium salt and a multidentate ligand having a tetrahedral structure (right). In contrast, regardless of the number of

metal coordination sites, ligands with a two-dimensional geometry lead to the formation of spheres and their aggregates (left).



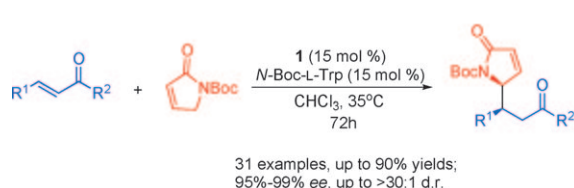
At arm's length: Branched DNA with exceptionally short sticky ends (see picture) assembles into a new material at temperatures where genomic DNA is fully denatured, if branching geometry and

linker rigidity favor crystallization. The process is shown by modeling and for synthetic material assembled from dilute aqueous buffer solution.

DNA-Based Assembly

A. Singh, M. Tolev, M. Meng, K. Klenin, O. Plietzsch, C. I. Schilling, T. Muller, M. Nieger, S. Bräse, W. Wenzel, C. Richert* — 3227 – 3231

Branched DNA That Forms a Solid at 95 °C



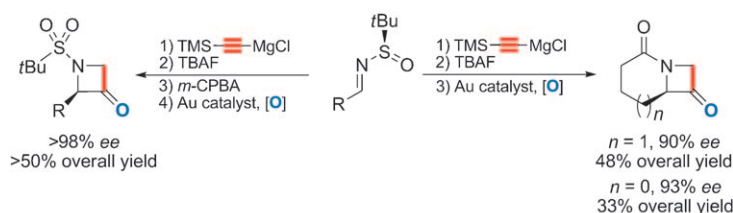
A direct line: A direct organocatalytic asymmetric vinylogous Michael addition of α,β -unsaturated γ -butyrolactams with α,β -unsaturated ketones has been developed (see scheme; Boc = *tert*-butoxycar-

bonyl, Trp = tryptophan, Ts = 4-toluene-sulfonyl). The resulting Michael products, 5-substituted 3-pyrrolidin-2-ones, could be obtained in excellent yields with excellent enantio- and diastereoselectivity.

Asymmetric Catalysis

H. Huang, Z. Jin, K. Zhu, X. Liang, J. Ye* — 3232 – 3235

Highly Diastereo- and Enantioselective Synthesis of 5-Substituted 3-Pyrrolidin-2-ones: Vinylogous Michael Addition under Multifunctional Catalysis



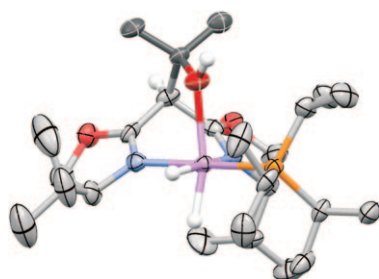
Chiral rings made easy: Chiral azetidin-3-ones have been easily prepared from chiral *N*-propargylsulfonamides, which in turn are readily accessible through chiral sulfinamide chemistry (see scheme).

Using *tert*-butylsulfonyl as the protecting group avoids unnecessary deprotection and reprotection steps, and allows its removal from the azetidine ring under acidic conditions.

N-Heterocycles

L. Ye, W. He, L. Zhang* — 3236 – 3239

A Flexible and Stereoselective Synthesis of Azetidin-3-ones through Gold-Catalyzed Intermolecular Oxidation of Alkynes



BOX of tricks: Facile, reversible, and diastereoselective functionalizations of methylene C–H bonds with carbonyl compounds have been observed within chiral bis(oxazoline)/iridium complexes (see structure; O red, N blue, P orange, Ir purple). These reactions are described and discussed together with the classic C–H oxidative additions to iridium that occur within these same compounds.

C–H Activation

M. R. Castillo, M. Martín, J. M. Fraile, J. A. Mayoral, E. Sola* — 3240 – 3243

Reversible Insertion of Aldehydes and Ketones into C_{sp^3} –H Bonds of Chiral Bis(oxazoline)/Iridium Complexes

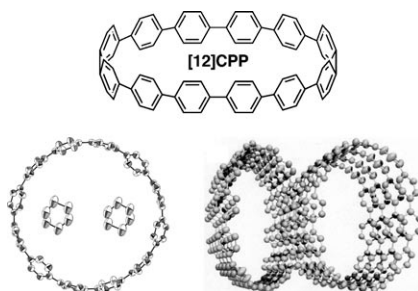


Carbon Nanorings

Y. Segawa, S. Miyamoto, H. Omachi,
S. Matsuura, P. Šenel, T. Sasamori,
N. Tokitoh, K. Itami* — 3244–3248



Concise Synthesis and Crystal Structure of [12]Cycloparaphenylene



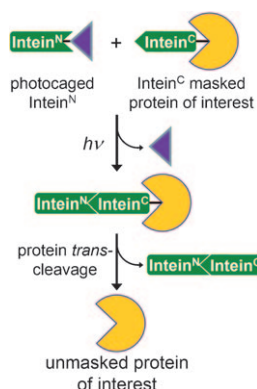
Crystal clear: The title macrocycle was constructed by a nickel-mediated shotgun macrocyclization. The X-ray crystallographic structure of [12]CPP revealed a circular structure incorporating two cyclohexane molecules within the ring. The [12]CPP molecules were also found to crystallize into tubular and herringbone structures.

Protein Activity

J. Binschik, J. Zettler,
H. D. Mootz* — 3249–3252



Photocontrol of Protein Activity Mediated by the Cleavage Reaction of a Split Intein



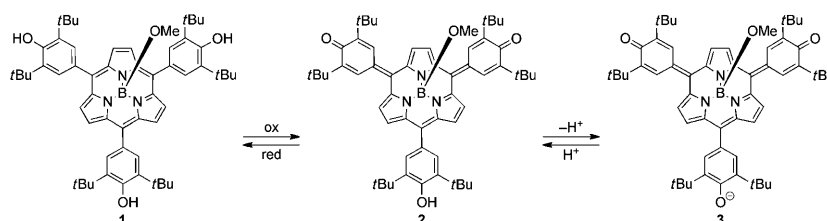
I want to break free: A photoactivatable split intein can be genetically fused to a protein of interest and used in potentially general ways to relay a phototrigger in a coupled fashion (see picture). The protein staphylocoagulase can be unmasked by light and thereby activates native prothrombin.

Porphyrinoids

S. Hayashi, J. Sung, Y. M. Sung,
Y. Inokuma, D. Kim,*
A. Osuka* — 3253–3256



Oxocyclohexadienylidene-Substituted Subporphyrins



Quinonoidal subporphyrin analogue 2 was synthesized by oxidation of *meso*-tris(3,5-di-*tert*-butyl-4-hydroxyphenyl)subporphyrin **1** (see scheme). Compound **2** was readily deprotonated to generate

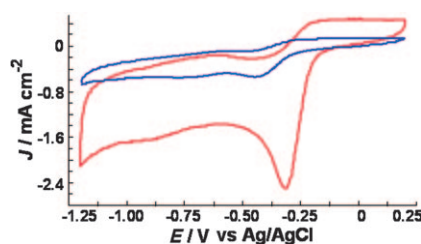
anionic species **3**. These three macrocycles were structurally characterized, including the full delocalization of the anionic charge in **3**.

Carbon Catalysis

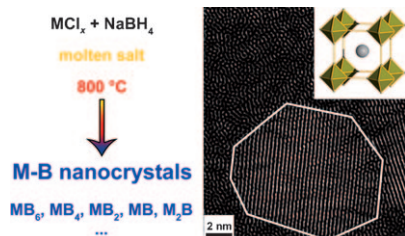
Z.-W. Liu, F. Peng,* H.-J. Wang, H. Yu,
W.-X. Zheng, J. Yang — 3257–3261



Phosphorus-Doped Graphite Layers with High Electrocatalytic Activity for the O₂ Reduction in an Alkaline Medium



Current events: A phosphorus-doped, graphite layer catalyst without any metal residue has been developed that shows high electrocatalytic activity, long-term stability, and excellent tolerance to cross-over effects of methanol in the oxygen reduction reaction. The oxygen reduction current densities of the glassy carbon (GC) electrode modified by the P-doped graphite (see red line in the picture) are much larger than those of the unmodified (blue line) and the GC electrode modified by a platinum-carbon catalyst (data not shown).

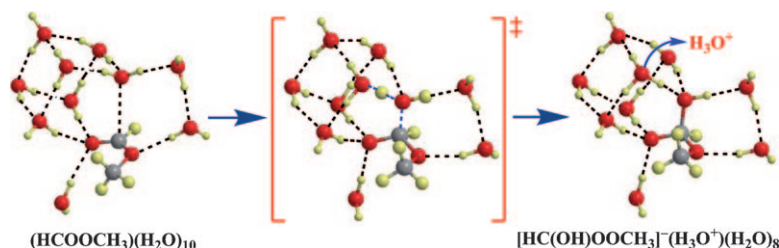


Mini B: An ionothermal process under relatively mild conditions ($500\text{--}900^\circ\text{C}$) provides the first versatile route towards nanocrystals of metal (Ca, Ce, Mo, Nb, Hf, Fe, Mn) hexaborides, tetraborides, diborides, and lower borides (see picture). Control over the nanoparticle size and the material texture is achieved to tune these functional materials.

Boride Nanoparticles

D. Portehault,* S. Devi, P. Beaunier, C. Gervais, C. Giordano, C. Sanchez, M. Antonietti ————— **3262–3265**

A General Solution Route toward Metal Boride Nanocrystals



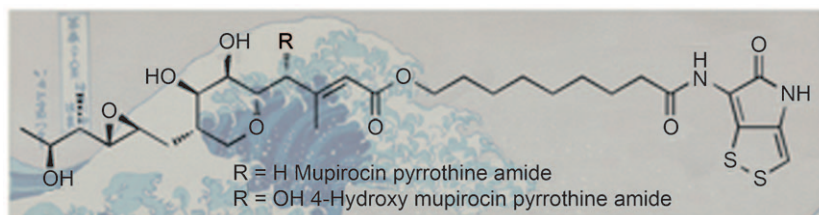
A step dance: Extensive cluster continuum model calculations verify that the stepwise hydration of a carbonyl group (see scheme: O red, H yellow, C gray) is more favorable than the widely suggested

concerted pathway. It is also shown that for reliable calculations on the water-mediated proton transfer a large basis set and a suitable cluster continuum model are required.

Hydration of Carbonyl Groups

B. Wang, Z. Cao* ————— **3266–3270**

Hydration of Carbonyl Groups: The Labile H_3O^+ Ion as an Intermediate Modulated by the Surrounding Water Molecules



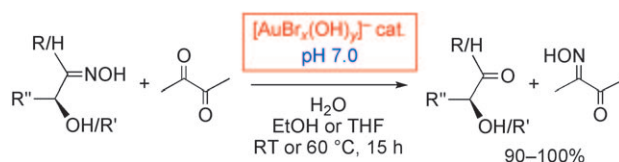
New drugs from marine bugs: The Japanese marine bacterium *Pseudoalteromonas* SANK73390 has been engineered to produce hybrid thiomarinol/pseudomonic acid compounds with potent activity against methicillin-resistant *Staphylococcus*

aureus (MRSA). Previously unreported mupirocin and pyrrothine metabolites were isolated from wild-type and mutant strains and from mutagenesis experiments with mutant strains.

Antibiotics

A. C. Murphy, D. Fukuda, Z. Song, J. Hothersall, R. J. Cox, C. L. Willis, C. M. Thomas, T. J. Simpson* ————— **3271–3274**

Engineered Thiomarinol Antibiotics Active against MRSA Are Generated by Mutagenesis and Mutasynthesis of *Pseudoalteromonas* SANK73390



Golden solution: A neutral solution of AuBr_3 , containing $[\text{AuBr}_3(\text{OH})_2]^-$ in equilibrium with $[\text{AuBr}_3(\text{OH})]^-$ and $[\text{AuBr}_4]^-$, promotes the chemoselective hydrolysis of robust oximes into carbonyl com-

pounds without racemization (see scheme). The food additive diacetyl acts as a NH_2OH -trapping agent, thus avoiding the formation of gold nanoparticles and allows the reaction to run catalytically.

Gold-Catalyzed Reactions

C. Isart, D. Bastida, J. Burés,* J. Vilarrasa* ————— **3275–3279**

Gold(III) Complexes Catalyze Deoximations/Transoximations at Neutral pH

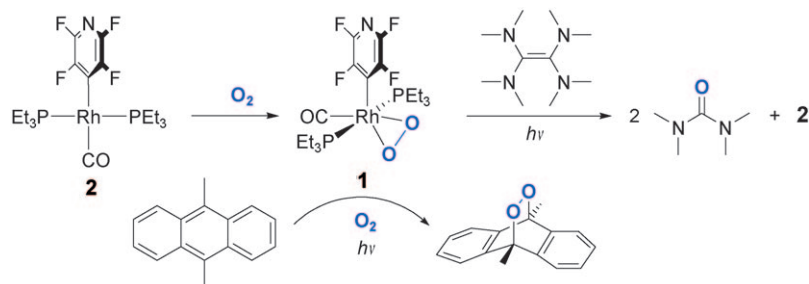


Peroxo Complexes

G. Meier, T. Braun* — 3280–3284



A Rhodium Peroxido Complex in Mono-, Di-, and Peroxygenation Reactions



A versatile peroxido complex: The rhodium peroxido complex **1**, which can be prepared from **2** and dioxygen, participates in mono-oxygenation of a phosphine and dioxygenation of tetrakis(dimethylamino)ethylene to give, respec-

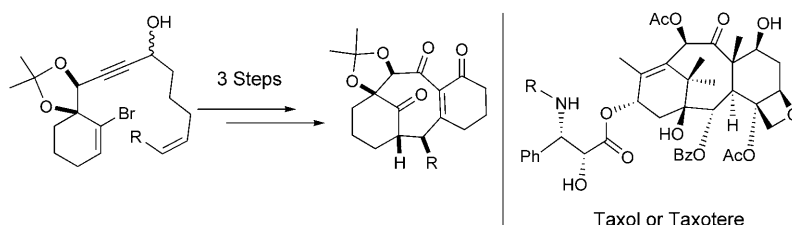
tively, phosphine oxide and a urea derivative, while peroxygenation of 9,10-dimethylanthracene to yield the anthracene endoperoxide takes place in the presence of dioxygen and substoichiometric amounts of **1** (see scheme).

Synthetic Methods

J. Petrignet, A. Boudhar, G. Blond, J. Suffert* — 3285–3289



Step-Economical Synthesis of Taxol-like Tricycles through a Palladium-Catalyzed Domino Reaction



A quick and easy way to produce tricycles related to the core structure of taxanes has been achieved using a palladium-catalyzed domino reaction (see scheme, Bz = benzoyl). These studies have been performed with function-oriented synthe-

sis in mind. An efficient route for the construction of new taxane scaffolds that could be decorated with various groups to achieve activities comparable or superior to taxol has been proposed.

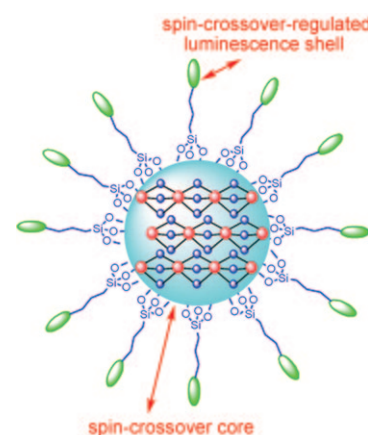
Functional Nanoparticles

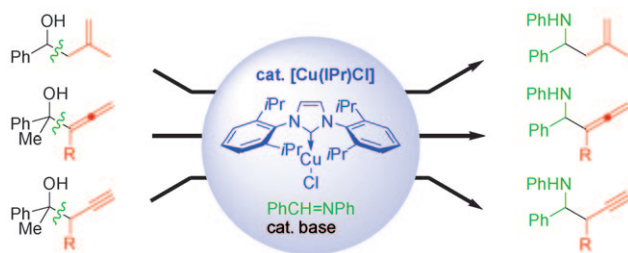
S. Titos-Padilla, J. M. Herrera,* X.-W. Chen, J. J. Delgado, E. Colacio* — 3290–3293



Bifunctional Hybrid SiO_2 Nanoparticles Showing Synergy between Core Spin Crossover and Shell Luminescence Properties

Let there be light: Hybrid SiO_2 nanoparticles with a spin-crossover polymer core and a luminescent shell have been synthesized (see picture). These nanoparticles exhibit a thermally induced low-spin (LS) \rightarrow high-spin (HS) transition that is accompanied by a drastic color change. This optical bistability tunes the luminescence properties of the fluorophores grafted on the surface of the materials.





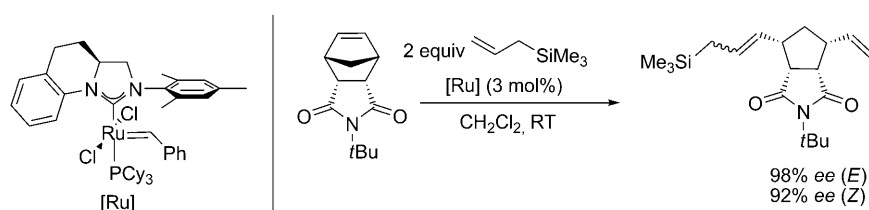
Cat. in the bag: The pictured copper complex can promote C–C bond cleavage through retro-allylation of homoallyl alcohols to form allylcopper species. This process is applicable to catalytic allylation

of aldehydes and imines with homoallyl alcohols. The method has also been extended to regioselective allenylation and propargylation of imines.

Copper Catalysis

M. Sai, H. Yorimitsu,*
 K. Oshima* ————— 3294 – 3298

Allyl-, Allenyl-, and Propargyl-Transfer Reactions through Cleavage of C–C Bonds Catalyzed by an N-Heterocyclic Carbene/Copper Complex: Synthesis of Multisubstituted Pyrroles



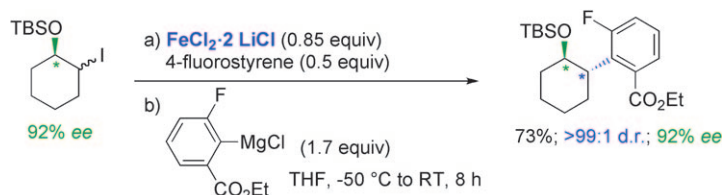
A bridge connects and efficiently transfers the chirality from the backbone of a N-heterocyclic carbene (NHC) to the metal center. The result is excellent enantio-

selectivities in the ruthenium-catalyzed, asymmetric ring-opening cross-metathesis of norbornenes with allyltrimethylsilane (see scheme).

Asymmetric Catalysis

A. Kannenberg, D. Rost, S. Eibauer,
 S. Tiede, S. Blechert* ————— 3299 – 3302

A Novel Ligand for the Enantioselective Ruthenium-Catalyzed Olefin Metathesis



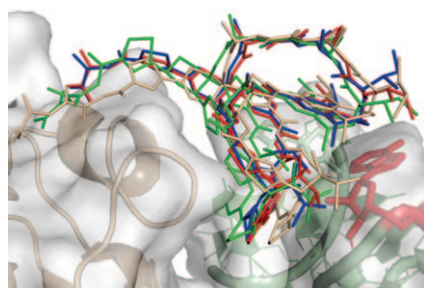
trans-2-Arylcycloalcohol derivatives are obtained in high diastereoselectivity by the iron-mediated cross-coupling of cyclic TBS-protected iodohydrines with aryl Grignard reagents (see scheme; TBS = *tert*-butyldimethylsilyl). The stereo-

convergent cross-coupling of a chiral TBS-protected 2-iodocyclohexanol provides the 2-arylcyclohexanols with no loss of stereochemical purity, and is a valuable alternative to the enantioselective opening of symmetrical epoxides.

Stereoselective Cross-Coupling

A. K. Steib, T. Thaler, K. Komeyama,
 P. Mayer, P. Knochel* ————— 3303 – 3307

Highly Diastereoselective Iron-Mediated C(sp²)–C(sp³) Cross-Coupling Reactions between Aryl Grignard Reagents and Cyclic Iodohydrine Derivatives



Structural probing: The activity of thioestrepton and derivatives with targeted shape changes was determined at their ribosomal binding site by using semisynthesis, NMR structure determination, docking (see picture), and biological evaluation in an integrated fashion. This combination revealed important elements of molecular recognition within the embedded pharmacophore of the target, a composite RNA–protein complex.

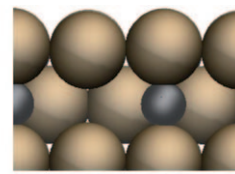
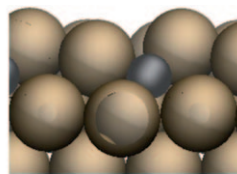
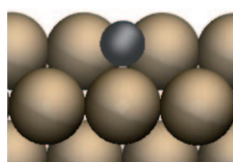
Antibiotics

H. R. A. Jonker, S. Baumann, A. Wolf,
 S. Schoof, F. Hiller, K. W. Schulte,
 K. N. Kirschner, H. Schwalbe,*
 H.-D. Arndt* ————— 3308 – 3312

NMR Structures of Thiostrepton Derivatives for Characterization of the Ribosomal Binding Site

Catalyst–Support Interactions

A. Rinaldi, J.-P. Tessonnier, M. E. Schuster, R. Blume, F. Girgsdies, Q. Zhang, T. Jacob,* S. B. Abd Hamid, D. S. Su,* R. Schlögl _____ 3313–3317



Dissolved Carbon Controls the Initial Stages of Nanocarbon Growth

Sneaked in: Carbon atoms from defective supports are incorporated in nickel nanoparticles at relatively low temperatures (for example in a Ni(100) surface; Ni brown, C black) The dissolved carbon not only modifies the electronic properties

of the metal but it also leads to a reconstruction of the nanoparticles. These findings may explain many of the differences in catalytic activity observed when supporting metals on carbon.

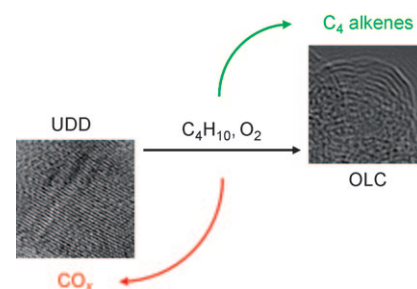
Metal-Free Catalysis

X. Liu, B. Frank, W. Zhang, T. P. Cotter, R. Schlögl, D. S. Su* _____ 3318–3322



Carbon-Catalyzed Oxidative Dehydrogenation of *n*-Butane: Selective Site Formation during sp^3 -to- sp^2 Lattice Rearrangement

Onions are a girl's best friend: While catalyzing the oxidative dehydrogenation of *n*-butane, ultradispersed nanodiamonds (UDD) are transformed into onionlike carbon (OLC, see picture). This surface-activated bulk transformation from sp^3 - to sp^2 -hybridized carbon atoms is concomitant with an enhanced product selectivity to the desired butenes. In addition, the synthesis of OLC is achieved at temperatures 600 K lower than reported so far.



Supporting information is available on www.angewandte.org (see article for access details).



A video clip is available as Supporting Information on www.angewandte.org (see article for access details).



This article is available online free of charge (Open Access)

Angewandte Chemie International Edition
WILEY InterScience®
DISCOVER SOMETHING GREAT

"Hot Papers" are chosen by the Editors for their importance in a rapidly evolving field of high current interest. A preview with the graphical abstracts of these articles can be found on the *Angewandte Chemie* homepage in Wiley InterScience at www.angewandte.org.

All articles in *Angewandte Chemie* are published online several weeks ahead of print. They are found under the "EarlyView" link on the journal's homepage in Wiley InterScience.

Angewandte

Service

Spotlight on Angewandte's Sister Journals _____ 3110–3112

Preview _____ 3323